Atmos. Chem. Phys. Discuss., 9, 22955–22992, 2009
www.atmos-chem-phys-discuss.net/9/22955/2009/

Atmospheric Chemistry and Physics Discussions

This discussion paper is/has been under review for the journal *Atmospheric Chemistry and Physics (ACP)*. Please refer to the corresponding final paper in *ACP* if available.

Eta-CMAQ air quality forecasts for O_3 and related species using three different photochemical mechanisms (CB4, CB05, SAPRC-99): comparisons with measurements during the 2004 ICARTT study

S. Yu[1], R. Mathur[1], G. Sarwar[1], D. Kang[2], D. Tong[3], G. Pouliot[1], and J. Pleim[1]

[1]Atmospheric Modeling and Analysis Division, National Exposure Research Laboratory, US Environmental Protection Agency, Research Triangle Park, NC 27711, USA
[2]Computer Science Corporation, Research Triangle Park, 79 T. W. Alexander Drive, NC 27709, USA

[3] Science and Technology Corporation, 10 Basil Sawyer Drive, Hampton, VA 23666-1393, USA

Received: 17 September 2009 – Accepted: 18 October 2009 – Published: 29 October 2009

Correspondence to: S. Yu (yu.shaocai@epa.gov)

Published by Copernicus Publications on behalf of the European Geosciences Union.

Abstract

A critical module of air quality models is the photochemical mechanism. In this study, the impact of three photochemical mechanisms (CB4, CB05, SAPRC-99) on the Eta-Community Multiscale Air Quality (CMAQ) model's forecast performance for O_3, and its related precursors has been assessed over the eastern United States with the observations obtained by aircraft (NOAA P-3 and NASA DC-8) flights, ship and two surface networks (AIRNow and AIRMAP) during the 2004 International Consortium for Atmospheric Research on Transport and Transformation (ICARTT) study. The results at the AIRNow surface sites show that for the observed $O_3 \geq 75$ ppb, CB05 has the best performance with the normalized mean bias (NMB) of 3.9%, followed by CB4 (NMB=−5.7%) and SAPRC-99 (NMB=10.6%), whereas CB4 has the best performance with the least overestimation for the observed $O_3 < 75$ ppb. On the basis of comparisons with aircraft P-3 measurements, there were consistent overestimations of O_3, NO_z, PAN and NO_y and consistent underestimations of CO, HNO_3, NO_2, NO, SO_2 and terpenes for all three mechanisms although the NMB values for each species and mechanisms were different. The results of aircraft DC-8 show that CB05 predicts the H_2O_2 mixing ratios most closely to the observations (NMB=10.8%), whereas CB4 and SAPRC-99 overestimated (NMB=74.7%) and underestimated (NMB=−25.5%) H_2O_2 significantly, respectively. For different air mass flows over the Gulf of Maine on the basis of the ship data, the three mechanisms have relatively better performance for O_3, isoprene and SO_2 for the clean marine or continental flows but relatively better performance for CO, NO_2 and NO for southwest/west offshore flows. The results of the O_3-NO_z slope over the ocean indicate that SAPRC-99 has the highest upper limits of the ozone production efficiency (ε_N) (5.8), followed by CB05 (4.5) and CB4 (4.0) although they are much lower than that inferred from the observation (11.8), being consistent with the fact that on average, SAPRC-99 produces the highest O_3, followed by CB05 and CB4, across all O_3 mixing ratio ranges.

ACPD

9, 22955–22992, 2009

1 Introduction

One of the most important components of air quality models (AQMs) is the photochemical mechanism which describes how volatile organic compounds (VOCs) and oxides of nitrogen (NO_x) interact to produce O_3 and other oxidants. Photochemical mechanisms were first used in AQMs more than 30 yr ago (e.g., Reynolds et al., 1973). Highly detailed and explicit photochemical mechanisms such as the Master Chemical Mechanism (MCM) (Jenkin et al., 1997), which includes over 2400 chemical species and over 7100 chemical reactions for 120 of the most important emitted organic compounds, exist. The chemistry of atmospheric systems involves reactions whose characteristic time scales vary by orders of magnitude, resulting in a set of nonlinear stiff ordinary differential equations (ODEs), the numerical integration of which often comprises a large fraction of the overall chemical transport model computational time (Mathur et al., 1998; McRae et al., 1982). Thus, for practical reasons, the representation of photochemical mechanism in AQMs employs different methods including various types of parameterizations, approximations and condensations (Dodge, 2000). Uncertainties in the model's chemical mechanisms can range to 30% or more when new techniques are applied to re-measure reaction rate constants and yields (Russell and Dennis, 2000).

Three of the most commonly used chemical mechanisms in current AQMs for both regulatory and research applications include the Carbon Bond 4 (CB4) (Gery et al., 1989), SAPRC-99 (Carter, 2000) and CB05 (an update to CB4, Yarwood et al., 2005). All three mechanisms have been evaluated against measurements from a large number of chamber experiments and have been demonstrated to be reasonably successful in predicting ozone and related species from complex mixtures in "typical" urban atmospheres (Gery et al., 1989; Yarwood et al., 2005; Carter, 2000). The Carbon Bond (CB) mechanisms mostly use lumped structure technique to condense the reactions of individual VOCs, whereas SAPRC mechanism uses lumped molecule technique to condense VOCs. In the lumped molecule technique, a generalized or surrogate species is used to represent similar organic compounds, whereas in the lumped

ACPD
9, 22955–22992, 2009

structure technique, organic compounds are grouped according to bond type. Given the fact that different chemical schemes can have different formulation of the reaction mechanism, different rate constants and temperature and pressure dependencies for the reactions (Kuhn et al., 1998), it is not surprising that different chemical mechanisms sometimes yield different prediction results. Several intercomparison studies of different chemical mechanisms have been performed with box and trajectory models, and 3-D AQMs over the last decade and the results have been summarized in detail by many investigators (Dunker et al., 1984; Stockwell, 1986; Jimenez et al., 2003; Gross and Stockwell, 2003; Kuhn et al., 1998; Luecken et al., 1999, 2008). For example, with box model calculation, Jimenez et al. (2003) compared seven different photochemical mechanisms (including LCC, CBM-IV, RADM2, EMEP, RACM, SAPRC-99 and CACM) and indicated that most chemical schemes yield similar O_3 mixing ratios. However, they also found significant discrepancies, mainly in predicted mixing ratios of HNO_3, HO_2 and total PAN among the model simulations, even under extremely simple situations. With the simulations of 3-D AQMs, Faraji et al. (2008) compared CB4 and SAPRC-99 in southeast Texas and found that for most urban areas, the CB4 and SAPRC-99 mechanisms yield similar results, but for 2000 summer in southeast Texas, the SAPRC-99 mechanism leads to O_3 mixing ratios by 30–45 pph higher than CB4. Faraji et al. (2008) attributed these discrepancies to differences in both reaction rate/stoichiometry parameters and condensation methods in the mechanisms. On the other hand, Luecken et al. (2008) recently examined the differences in predictions of O_3 and its O_3 precursors among CB4, CB05 and SAPRC-99 in a 3-D MM5-CMAQ model over the continental US. They show that the predicted O_3 mixing ratios are similar for most of the US, but statistically significant differences occur over many urban areas and the central US among the predictions by the three mechanisms, depending on location, the VOC/NO_x ratio, and precursor concentrations. They also found that on average, SAPRC-99 predicts the highest O_3, followed by CB05 and CB4.

In this study, we compare the CB4, CB05 and SAPRC-99 mechanisms by examining the impact of these different chemical mechanisms on the Eta-CMAQ air quality

ACPD
9, 22955–22992, 2009

forecast model simulations for O_3 and its related precursors over the eastern US through comparisons with the intensive observational data obtained during the 2004 International Consortium for Atmospheric Research on Transport and Transformation (ICARTT) study. The 2004 ICARTT experiment provided a comprehensive set of measurements of chemical constituents, both from surface and aircraft based platforms, which can be used to examine in detail the impact of chemical mechanisms from a multi-pollutant perspective, both in terms of their surface concentrations as well as vertical structure. This aspect constitutes the primary difference of this study from the previous comparative analyses of these mechanisms. The objectives of this study are three-fold. First, the influence of three photochemical mechanisms on the simulated ground-level O_3 over the eastern US during 2004 ICARTT period is examined through comparison with observations from the US EPA AIRNow network. Second, the impact of three photochemical mechanisms on the Eta-Community Multiscale Air Quality (CMAQ) model's ability to simulate O_3, its related chemical species (CO, NO, NO_2, NO_y, H_2O_2, CH_2O, HNO_3, PAN, isoprene, terpenes) is assessed over the eastern United States with the observations obtained by aircraft (NOAA P-3 and NASA DC-8) flights and ship during the 2004 ICARTT study. Third, on the basis of the intensive datasets obtained at the four Atmospheric Investigation, Regional Modeling, Analysis, and Prediction (AIRMAP) surface sites, a variety of tests were used to examine the influence of three photochemical mechanisms on simulating the processes governing the distributions of tropospheric O_3.

2 Description of the photochemical mechanisms, Eta-CMAQ model and observation database

2.1 Photochemical mechanisms

Detailed description of CB4, CB05 and SAPRC-99 chemical mechanisms (species and reaction rates) and their evaluations against smog chamber experimental data can be

ACPD
9, 22955–22992, 2009

found in Gery et al. (1989), Yarwood et al. (2005) and Carter (2000), respectively. Luecken et al. (2008) previously summarized the general characteristics of the three mechanisms used in this study; a brief summary relevant to this study is presented here. The version of CB4 in CMAQ (http://www.cmaq-model.org) has 46 species (30 organic species) and 96 reactions (45 inorganic reactions). In contrast, CB05, an updated version of the CB4, includes 59 species and 156 reactions, with updated reaction rate constants, additional inorganic reactions and more organic species relative to CB4. Both CB4 and CB05 mostly use the lumped-structure technique to condense the organic chemistry. On the other hand, SAPRC-99 has 80 species and 214 reactions and uses a lumped molecule approach to condense the organic chemistry, i.e., surrogate species is used to represent similar organic compound. Tables 1 and 2 compares the reaction rates of inorganic and organic species (also see Table 6 for more organic reactions) at 298 K and 1 atm, respectively, for the three mechanisms. Inorganic chemistry describes the chemistry of O_3, various NO_x species, H_2O_2, OH and HO_2 radicals, CO, HNO_3, HNO_2, HNO_4 and PNA. Organic chemistry includes the chemistry of formaldehyde, higher molecular weight aldehydes, alkanes, alkenes, aromatics, isoprene, terpene, ketone, and other organic compounds. As can be seen, there are many differences among CB4, CB05 and SAPRC-99 chemical mechanisms. SAPRC-99 includes more detailed organic chemistry than Carbon Bond mechanisms as SAPRC-99 was developed with the additional capability of representing reactions of a wide variety of individual VOCs (Carter, 1999). Updates to inorganic chemistry in CB05 compared to CB4 mechanism include (Yarwood et al., 2005): 1) updated rate constants based on recent (2003-2005) IUPAC and NASA evaluations, 2) an extended inorganic reaction set for urban to remote tropospheric conditions, 3) NO_x recycling reactions to represent the fate of NO_x over multiple days. Updates to organic chemistry in CB05 compared to CB4 mechanism include (Yarwood et al., 2005): 1) explicit organic chemistry for methane and ethane, 2) explicit methylperoxy radical methyl hydroperoxide and formic acid, 3) lumped higher organic peroxides, organic acids and peracids, 4) internal olefin (R–HC=CH–R) species called IOLE, 5) higher aldehyde species ALDX making ALD2

explicitly acetaldehyde, 6) higher peroxyacyl nitrate species from ALDX called PANX. As analyzed by Luecken et al. (2008), the reasons for CB05 to produce more O_3 relative to CB4 include 1) the ALDX (aldehydes with more than two carbons) species in CB05 can produce about 50% more conversions of NO to NO_2, 2) the photolysis rate of ALDX in CB05 is higher compared to ALD2, leading to higher production of HO_x, 3) the additional acyl peroxy radicals (CXO3) in CB05 (e.g., CB05 uses two species (acetyl peroxy radical (C2O3) and other acyl peroxy radicals (CXO3) while CB4 only uses one species to represent all acyl peroxy radicals (C2O3)) can produce 50% more conversions of NO to NO_2 than C2O3; this effect is apparent in the reactions of alkenes, including isoprene, with O_3 and NO_3, 4) CB05 uses methyl peroxy radical (MEO2) to replace the alkyl peroxy radical operator (XO2) in some reactions to better represent reactions under low NO_x conditions, 5) CB05 adds a model species to represent internal alkenes which allowed to react with O_3 and can change the temporal production of O_3, 6) CB05 allows HNO_3 and organic nitrate to photolyze and produce HO_x and NO_2, providing additional organic radicals.

2.2 Eta-CMAQ forecast model

The developmental Eta-CMAQ air quality forecasting system for O_3, created by linking the Eta model (Rogers et al., 1996) and the CMAQ Modeling System (Byun and Schere, 2006), was applied over a domain encompassing the eastern US (see Fig. 1) during summer 2004. The detailed description of model configurations can be found in Yu et al. (2007). The Eta model provided the meteorological fields for input to CMAQ. The model domain has a horizontal grid spacing of 12 km with twenty-two vertical layers between the surface and 100 mb. The boundary conditions for various species were based on a static vertical profile that was uniformly applied along all lateral boundaries. The species profiles are representative of continental "clean" conditions except O_3 whose lateral boundary conditions are derived from the Global Forecast System (GFS) model. The primary Eta-CMAQ model forecast for next-day is based on the current day's 12:00 UTC Eta simulation cycle. The area source emissions are based

on the 2001 National Emission Inventory (NEI). The point source emissions are based on the 2001 NEI with SO_2 and NO_x projected to 2004 on a regional basis using the Department of Energy's 2004 Annual Energy Outlook issued in January of 2004. The mobile source emissions were generated by EPA'S MOBILE6 model using 1999 vehicle miles traveled (VMT) data and a fleet year of 2004. Daily temperatures from the Eta model were used to drive the inputs into the MOBILE6 model using a nonlinear least squares relationship described in Pouliot (2005). The biogenic emissions are calculated using Biogenic Emissions Inventory System (BEIS) version 3.12. The CB4, CB05 and SAPRC-99 chemical mechanisms as described in Sect. 2.2 have been used to represent photochemical reaction pathways in the three cases.

2.3 Observation database

The hourly, near real-time observed O_3 data at 614 sites in the eastern US are available from the US EPA's AIRNow network (Fig. 1), resulting in nearly 1.2 mill total hourly O_3 observations for the study period. From 1 July–15 August 2004, measurements of vertical profiles of O_3, its related chemical species (CO, NO, NO_2, H_2O_2, CH_2O, HNO_3, SO_2, PAN, isoprene, terpenes) were carried out by instrumented aircraft (NOAA P-3 and NASA DC-8) deployed as part of the 2004 ICARTT field experiment. The detailed instrumentation and protocols for measurements are described in http://www.esrl.noaa.gov/csd/ICARTT/fieldoperations/. The flight tracks of P-3, DC-8, and ship are presented in Fig. 2. Four sites of the AIRMAP (DeBell et al., 2004; Mao and Talbot, 2004) provided continuous measurements of O_3 and related photochemical species as well as meteorological parameters during the study; the sites include Castle Springs (CS) (43.73° N, 71.33° W), New Hampshire (NH), Isle of Schoals (IS) (42.99° N, 69.33° W), Maine, Mount Washington Observatory (MWO) (44.27° N, 71.30° W), NH, and Thompson Farm (TF) (43.11° N, 70.95° W), NH. The comparison of the model results for three mechanisms during the period of 15 July–18 August 2004 is examined in this study.

3 Results and discussion

3.1 O_3 comparison at the AQS sites

To gain additional insights into the model performance, the normalized mean bias (NMB) values (Yu et al., 2006) as a function of the different observed O_3 mixing ratio ranges are calculated for three mechanisms as displayed in Fig. 1. As can be seen, for the O_3 mixing ratios greater than 75 ppb, CB05 exhibits the best performance with the NMB of 3.9%, followed by CB4 (NMB=−5.7%) and SAPRC-99 (NMB=10.6%). In contrast, for O_3 mixing ratios less than 75 ppb, CB4 exhibited the least overestimation amongst the three mechanisms at the low mixing ratio ranges; CB05 and SAPRC-99 produce more O_3 for all O_3 mixing ratio ranges than CB4 (see Fig. 1). As analyzed by Yu et al. (2007), one of the reasons for the overestimation of the observations in the low O_3 mixing ratio ranges could be indicative of titration by NO in urban plumes that the model does not resolve because most of the AIRNow sites are located in urban areas. Another one is also because of the significant overestimation in areas of cloud cover mainly caused by the unrealistic vertical transport of excessive amounts of high O_3 concentrations near the tropopause to the ground associated with downward entrainment in CMAQ's convective cloud scheme (Yu et al., 2007). The spatial distributions of NMB values for three mechanisms indicate that large overestimation of the observed daily max 8-h O_3 mixing ratios was in the northeast where very low O_3 mixing ratios were observed for all three mechanisms (not shown). Spatially, SAPRC-99 is more similar to CB05 with the except that SAPRC-99 has slightly more overpredictions.

3.2 Vertical profile comparisons for different species

To compare the modeled and observed vertical profiles, the observed and modeled data were grouped according to the model layer for each day and each flight: that is, both observations and predictions were averaged along the aircraft transect according to layer height, representing the average conditions encountered over the study

ACPD
9, 22955–22992, 2009

area. The aircraft flight tracks in Fig. 2 show that observations onboard the P-3 cover a regional area over the northeast around NY and Boston from 0 to ~5 km altitudes, whereas the DC-8 aircraft covers a broader regional area over the eastern US between 0 and 12 km altitudes. Figures 3–5 present observed and modeled (CB4, CB05, SAPRC-99) vertical profiles for O_3, CO, SO_2, NO_x, NO, NO_2, HNO_3, NO_y, NO_2+O_3, HCHO, terpenes, isoprene, PAN, and H_2O_2 on the daily basis during the 2004 ICARTT period. Table 3 summarizes the results of comparison for all observation and model data during the 2004 ICARTT period.

As shown in Figs. 3 and 5, and Table 3, all three mechanisms tend to consistently overestimate O_3 from low altitude to high altitude with the highest for SAPRC-99, followed by CB05 and CB4, similar to trends noted relative to AIRNow measurement at the surface, although they reproduce the composite vertical variation patterns of O_3 well. All three mechanisms tend to overestimate more in the upper layers at altitude >6 km on the basis of DC-8 observations (see Fig. 5) due to effects of the lateral boundary conditions derived from the Global Forecast System (GFS) model and coarse model resolution in the free troposphere (Yu et al., 2007). Figures 3–5 and Table 3 also indicate that there are noticeable many consistence and discrepancies for different species among three chemical mechanisms. Noticeable among these are consistent overestimations of O_3, NO_z, PAN, NO_y, and O_3+NO_z and consistent underestimations of CO, HNO_3, NO_2, NO, SO_2, and terpenes relative to the P3 observations. There were consistent overestimations of O_3, HNO_3, and HCHO and consistent underestimations of CO, NO_2, SO_2, and NO relative to DC-8 observations for all three mechanisms although the NMB values for each species and mechanism are somehow different as listed in Table 3. One reason for the consistent underestimations of CO relative to both P3 and DC8 observations for the three model configurations can be attributed to the inadequate representation of the transport of pollution associated with biomass burning from outside the domain, especially from large Alaska forest fires during this period (Yu et al., 2007; Mathur, 2008).

ACPD
9, 22955–22992, 2009

In terms of the NMB values for each species relative to P3 observations in Table 3, CB4 has the relative better performance for O_3 and HNO_3, whereas CB05 has the relative better performance on CO, NO_2, SO_2, and NO_x. In general, CB05 and SAPRC-99 yield similar results for different species. The speciation of NO_y in different mechanisms are different, i.e., CB4: NO_y=NO+NO_2+NO_3+2N_2O_5+HONO+HNO_3+PAN+PNA+NTR, CB05: NO_y=NO+NO_2+NO_3+2N_2O_5+HONO+HNO_3+PAN+PNA+NTR+PANX, and SAPRC-99: NO_y=NO+NO_2+NO_3+2N_2O_5+HONO+HNO_3+HNO_4+PAN+PAN2+PBZN+MA_PAN+BZNO2_O+NPHE. Despite the fact that CB4 apportions PAN (peroxyacetyl nitrate) and homologs (peroxyprionyl nitrate and larger compounds) differently from the CB05 and SAPRC-99 (Luecken et al., 2008), both CB4 and CB05 overestimated observed PAN from low to high altitudes (see Fig. 4) by about a factor of 2 while SAPRC-99 results are more close to the observations (see Table 3). There are the consistent underestimations of NO_x relative to both P3 and DC-8 observations (See Table 3 and Figs. 3 and 4) for all three mechanisms, being in agreement with Singh et al. (2007). This is due to the fact that the aircraft and lightning NO emissions are not included in the current model emission inventory. Ridley et al. (2005) suggested that cloud-to-cloud discharges may be a far greater source of NO_x than what has traditionally been believed. Three mechanisms slightly underestimated HNO_3 relative to P3 observations while they slightly overestimated HNO_3 relative to DC-8 observation as shown in Table 3. One of reasons for this different performance is because of different areas measured by P3 and DC-8 as shown Fig. 2.

On the basis of DC-8 observations, CB05 has relative better performance for H_2O_2, and CO compared to those of CB4 and SAPRC-99. H_2O_2 and hydroperoxide radical (HO_2) are photochemical products and affected by the levels of chemical components such as NO_x, CO, methane and non-methane hydrocarbons (Lee et al., 2000). Kuhn et al. (1998) pointed out that H_2O_2 and organic peroxides chemistry is a weak point in most mechanisms due to the fact that there are many complex reactions and possibly important unknowns like the incorrect use of the HO_2+HO_2 rate constant and different treatment of the peroxy radical interactions. Among the three mechanisms, the

ACPD
9, 22955–22992, 2009

H_2O_2 mixing ratios from CB05 are the closest to the observations with a NMB value of 10.8%, whereas CB4 significantly overestimated the H_2O_2 mixing ratios from low to high altitudes (see Fig. 5) with the NMB value of 74.7% (see Table 3) due to the fact that the H_2O_2 formation rate in CB4 is 62% higher than CB05 or SAPRC-99 (Luecken et al., 2008). On the other hand, SAPRC-99 underestimated H_2O_2 mixing ratios with a NMB value of −25.5%. Comparing to SAPRC-99, CB05 can produce more new HO_2, enhancing formation of H_2O_2 as pointed out by Luecken et al. (2008). The different model performance for the same species relative to P3 and DC-8 observations can be attributed to the difference in the studying areas of P3 and DC-8 as indicated in Fig. 2.

Biogenic monoterpene and isoprene emission rates are high over the coniferous forests of northeastern North America, especially in the summer months (Guenther et al., 2000). Isoprene is the most significant biogenic compound regarding photochemistry and terpene is a significant gas precursor for the formation of biogenic secondary organic aerosols (SOA). Isoprene is highly reactive in the atmosphere with a relative short lifetime compared to other reactive VOCs. Table 2 shows that all three mechanisms consider the reactions of isoprene with atomic oxygen, OH radicals, NO_3 radicals, and O_3 although the reaction products and propagation reactions are different amongst the mechanisms. The results in Fig. 4 show that three mechanisms have similar performance for isoprene with significant overestimation at altitudes between ~200 and 300 m but slight underestimation above it. On average for all data as summarized in Table 3, CB05 has slightly better results for isoprene with the NMB value of 5.5%, whereas CB4 and SAPRC-99 have the negative NMB values of −6.0% and −8.4%, respectively. A close inspection of Fig. 4 shows that CB05 has slightly higher isoprene mixing ratios at the high altitudes (>Layer 5) than CB4 and SAPRC-99. On the other hand, three mechanisms systematically underestimated the observed terpenes by more than a fact of 2 from low to high altitudes except at the layer 3 (~200 m) where the mean results of three mechanisms are close to the observations due to high model terpenes mixing ratios at layer 3 on 7/22 when the P3 observations took place over the northeastern part as indicated in Fig. 2. Improvement of the VOC emission inventory

ACPD
9, 22955–22992, 2009

is recommended in order to provide better model results for these species.

3.3 Time series comparison over the ocean with the Ronald H. Brown ship observations

The cruise tracks of the NOAA ship Ronald H. Brown of Fig. 2 shows that most of ship's time was spent sampling along the coast of New Hampshire, Massachusetts and Maine. The time-series of the observations and models (CB4, CB05 and SAPRC-99) for different species (O_3, O_3+NO_2, CO, NO_y, NO_2, NO, PAN, SO_2, and isoprene) along the ship tracks during the ICARTT period are shown in Fig. 6. As analyzed by Yu et al. (2007), the air mass flow patterns sampled in the Gulf of Maine can be divided into two groups for our study period: 1) offshore flow from the southwest and west where are significantly affected by anthropogenic sources from the Washington, DC/New York City/Boston urban corridor and biogenic emissions in New Hampshire and Maine, and 2) relatively clean marine and continental flow from east, south, north and northwest. On days with the southwest/west offshore flows such as 10 July, 15–17 July, and 20–23 July, 29 July–1 August, 3–4 August, 8–12 August, and 16–17 August, measured concentrations for each species were clearly seen above the background values. The east/north/northwest/south clean marine or continental flows impacted the ship observations on days 11–13 July, 18 July, and 25–28 July and 5–7 August which were characterized by low mixing ratios of O_3, CO, NO_y, SO_2, and NO_x. Table 4 summarizes the mean results for these two different flows on the basis of wind fields observed by High-Resolution Doppler Lidar (HRDL) (Yu et al., 2007). As can be seen, all three mechanism model configurations exhibit relatively better model performance for the clean marine or continental flows for O_3, O_3+NO_2, isoprene, and SO_2 compared to southwest/west offshore flows. On the other hand, three mechanisms exhibit relatively better model performance for CO, NO_2, and NO for southwest/west offshore flows. The clean marine or continental flows have significantly lower mixing ratios than southwest/west polluted flows for all species except NO and PAN on the basis of observations. The three mechanisms have very similar performance for the clean marine or continental

ACPD
9, 22955–22992, 2009

flows with general underestimations for all species except O_3 as shown Table 4 due to the fact that the mixing ratios of all those species are close to the background in these clean flows. In contrast, all three mechanism model configuration exhibit consistent overestimations of SO_2, PAN, NO_y, and O_3 for the southwest/west polluted flows.

In terms of the NMB values for each species in Table 4, three mechanisms reproduced the observations of CO, NO_2, and NO in the southwest/west polluted flows well with the NMB value<±20%. Comparing the results of Tables 4 and 3 for each species, the model performance statistics for the southwest/west polluted flow conditions are similar to those for the aircraft measurement comparisons. For example, in the southwest/west polluted flows, all three mechanisms tend to consistently overestimate O_3 with the highest for SAPRC-99, followed by CB05 and CB4, and three mechanisms tend to consistently overestimate NO_y and PAN with the slightly better performance for SAPRC-99. Also noticeable in these comparisons is significant overestimation of SO_2 but underestimation of isoprene during the southwest/west polluted flows. This suggests that the model may have overestimated some of emission sources of SO_2 from urban plumes over Washington, DC/New York City/Boston areas and underestimated biogenic emissions of isoprene.

The upper limits of the ozone production efficiency (ε_N) values can be estimated by the O_3-NO_z (NO_z=NO_y–NO_x) slope because NO_z species (primarily HNO_3) are removed from the atmosphere more rapidly than O_3 (Yu et al., 2007). Following Arnold et al. (2003), both modeled and observed O_3-NO_z slopes are obtained for only observational data with $[O_3]/[NO_x]>46$. The results of Table 4 reveal that the ε_N values of three mechanisms are much lower than the corresponding observation (11.8) with the highest for SAPRC-99 (5.8), followed by CB05 (4.5) and CB4 (4.0), whereas the intercepts of O_3-NO_z relationships for the three mechanisms are higher than the observation, indicating too high background O_3 mixing ratios in the model. The ε_N values of SAPRC-99 (5.8), CB05 (4.5) and CB4 (4.0) are consistent with the fact that SAPRC-99 produces the highest O_3, followed by CB05 and CB4 as previously analyzed. Too high NO_z mixing ratios in the model indicate that all three chemical mechanisms still produce more

ACPD
9, 22955–22992, 2009

terminal oxidized nitrogen products than inferred from observations, thereby contributing in part to the noted underestimation of ε_N.

3.3.1 Comparisons at the AIRMAP sites

Table 5 lists the comparison of observations and three mechanisms (CB4, CB05 and SAPRC-99) for different species (O_3, CO, NO, NO_y, and SO_2) at the four AIRMAP (CS, IS, MWO and TF) sites on the basis of hourly time-series data during the 2004 ICARTT period. As can be seen, there are several consistent features in the model performance of three mechanism model configurations at each site. All three mechanisms underestimate NO, and CO but overestimate O_3 at all four sites. The three mechanisms consistently overestimated NO_y at the CS, and TF sites but underestimated NO_y at the MWO site. Compared to the other sites, relative poor model performance for several species is noted at the MWO site (the highest mountain (1916 m) in the northeastern US). This, in part, arises from the inability of the model to capture the inherent sub-grid variability at this location. The models usually misrepresent mountain sites because they essentially sample free tropospheric air while the models can't resolve the terrain. Overall, CB4 has the smallest NMB values for O_3 based on the entire hourly data, whereas SAPRC-99 has the better results for NO_y at the CS and TF sites. This also is in agreement with the previous results of P-3.

4 Summary and conclusions

A rigorous comparison of three photochemical mechanisms (CB4, CB05 and SAPRC-99) for the Eta-CMAQ air quality forecast model for O_3 and its related precursors has been carried out by comparing the model results with intensive observations over the eastern United States obtained during the 2004 ICARTT study. All three photochemical mechanisms are used as part of chemical transport models in the Eta-CMAQ air quality forecast model. The main conclusions of the comparison results are summarized

ACPD
9, 22955–22992, 2009

below. The comparisons with measurements at the AIRNow surface sites show that SAPRC-99 predicts the highest O_3 mixing ratios, followed by CB05 and CB4 for all O_3 mixing ratio ranges and that relative to observations for the O_3 mixing ratios ≥75 ppb, CB05 has the best performance with NMB=3.9%, followed by CB4 (NMB=−5.7%) and SAPRC-99 (NMB=10.6%), whereas CB4 has the best performance for observed O_3 mixing ratios <75 ppb. On the basis of vertical results from P-3 and DC-8 aircraft, all three mechanisms tend to consistently overestimate O_3 from low altitude to high altitude with the highest for SAPRC-99, followed by CB05 and CB4 similar to trends noted at the AIRNow surface sites. On the basis of P-3 observations, there were consistent overestimations of O_3, NO_z, PAN, and NO_y, and consistent underestimations of CO, HNO_3, NO_2, NO, SO_2 and terpenes for three mechanisms although the NMB values for each species and mechanism are somehow different. On the basis of DC-8 observations, CB05 has relative better performance on HNO_3, H_2O_2, and CO than the CB4 and SAPRC-99. Among three mechanisms, CB05 predictions of H_2O_2 are the closest to the observations with NMB=10.8%, whereas CB4 significantly overestimates H_2O_2 with NMB=74.7% and SAPRC-99 significantly underestimates H_2O_2 with NMB=−25.5%. This is due to the fact that the H_2O_2 formation rate in CB4 is 62% higher than CB05, and relative to SAPRC-99, CB05 can produce more new HO_2, enhancing formation of H_2O_2. The three mechanisms estimated isoprene reasonably well with NMB<±10% but systematically underestimated the observed terpenes by more than a factor of 2 most of time.

The capability of the three mechanisms to reproduce the observed pollutants over the ocean areas (Gulf of Maine) was found to be dependent on the offshore flow types. The three mechanisms exhibit relatively better performance for O_3, isoprene and SO_2 for the clean marine or continental flows but relatively better performance for CO, NO_2 and NO for southwest/west offshore flows. Model performance during southwest/west polluted flow conditions was similar to that noted for aircraft measurements. According to the ship data, the upper limits of the ozone production efficiency (ε_N) values estimated on the basis of the O_3-NO_z slope are 5.8, 4.5, and 4.0 for SAPRC-99, CB05

ACPD
9, 22955–22992, 2009

and CB4, respectively, much lower than the observation (11.8). This is also consistent with the fact that SAPRC-99 produces the highest O_3, followed by CB05 and CB4. Too high NO_z mixing ratios in the model also contribute in part to the noted underestimation of ε_N.

In light of the uncertainties in the photochemical mechanisms, prognostic model forecasts of meteorological fields and emissions, the overall performance of the three mechanisms can be considered to be reasonable. On the other hand, given the fact that three mechanisms use different method to condense the organic chemistry and have different number of species, leading to difficulty for defining completely equivalent emissions as well as complicating comparisons of chemistry in three mechanisms, it is not obviously possible to prove which one is "correct" for O_3 and its related precursor predictions. However, it is important and necessary that the older chemical mechanisms be revised periodically to be consistent with current scientific knowledge. Therefore, the CB05 mechanism can be considered to be superior to the CB4 mechanism because it has better treatment of both inorganic and organic reactions and more number of species according to the state-of-the-science than CB4.

Acknowledgements. The authors would like to thank S. T. Rao and D. Luecken for the constructive and very helpful comments that led to a substantial strengthening of the content of the paper. We thank J. McQueen, P. Lee, and M. Tsidulko for collaboration and critical assistance in performing the forecast simulations. We are grateful to the 2004 ICARTT investigators for making their measurement data available. The AIRMAP data were obtained from the University of New Hampshire's AIRMAP Observing Stations that are supported through NOAA's Office of Oceanic and Atmospheric Research. The United States Environmental Protection Agency through its Office of Research and Development funded and managed the research described here. It has been subjected to Agency's administrative review and approved for publication.

References

Arnold, J. R., Dennis, R. L., and Tonnesen, G. S.: Diagnostic evaluation of numerical air quality models with specialized ambient observations: testing the Community Multiscale Air Quality modeling system (CMAQ) at selected SOS 95 ground sites, Atmos. Environ., 37, 1185–1198, 2003.

Byun, D. W. and Schere, K. L.: Review of the governing equations, computational algorithms, and other components of the models-3 Community Multi-scale Air Quality (CMAQ) modeling system, Appl. Mech. Rev., 59, 51–77, 2006.

Carter, W. P. L.: Implementation of the SAPRC-99 chemical mechanism into the models-3 framework, Report to the United States Environmental Protection Agency, http://www.engr.ucr.edu/~carter/pubs/s99mod3.pdf, 2000.

Dennis, R. L., Byun, D. W., Novak, J. H., Gallupi, K. J., Coats, C. J., and Vouk, M. A.: The next generation of integrated air quality modeling: EPA's Models-3, Atmos. Environ., 30(12), 1925–1938, 1996.

Dodge, M. C.: A comparison of photochemical oxidant mechanisms, J. Geophys. Res., 94, 5121–5136, 1989.

Dunker, A. M., Kumar, S., and Berzins, P. H.: A comparison of chemical mechanisms used in atmospheric models, Atmos. Environ., 18, 311–321, 1984.

Faraji, M., Kimura, Y., McDonald-Buller, E., and Allen, D.: Comparison of the Carbon Bond and SAPRC photochemical mechanisms under conditions relevant to southeast Texas, Atmos. Environ., 42, 5821–5836, doi:10.1016/j.atmosenv.2007.07.048, 2008.

Gery, M. W., Whitten, G. Z., Killus, J. P., and Dodge, M. C.: A photochemical kinetics mechanism for urban and regional scale computer modeling, J. Geophys. Res., 94(D10), 12925–12956, 1989.

Guenther, A., Geron, C., Pierce, T., Lamb, B., Harley, P., and Fall, R.: Natural emissions of non-methane volatile organic com-pounds, carbon monoxide, and oxides of nitrogen from North America, Atmos. Environ., 34(12–14), 2205–2230, 2000.

Gross, A. and Stockwell, W.: Comparison of the EMEP, RADM2 and RACM mechanisms, J. Atmos. Chem., 44, 151–170, 2003.

Jenkin, M. E., Saunders, S. M., and Pilling, M. J.: The tropospheric degradation of volatile organic compounds: a protocol for mechanism development, Atmos. Environ., 31, 81–104, 1997.

Jimenez, P., Baldasano, J. M., and Dabdub, D.: Comparison of photochemical mechanisms for air quality modeling, Atmos. Environ., 37, 4179–4194, 2003.
Kuhn, M., Builtjes, P. J. H., Poppe, D., Simpson, D., Stockwell, W. R., Andersson-Skold, Y., Baart, A., Das, M., Fiedler, F., Hov, O., Kirchner, F., Makar, P. A., Milford, J. B., Roemer, M. G. M., Ruhnke, R., Strand, A., Vogel, B., and Vogel, H.: Intercomparison of the gas-phase chemistry in several chemistry and transport models, Atmos. Environ., 32, 693–709, 1998.
Lee, M., Heikes, B. G., and O'Sullivan, D. W.: Hydrogen peroxide and organic hydroperoxide in the troposphere: a review, Atmos. Environ., 34, 3475–3494, 2000.
Luecken, D. J., Tonnesen, G. S., and Sickles, J. E.: Differences in NO_y speciation predicted by three photochemical mechanisms, Atmos. Environ., 33, 1073–1084, 1999.
Luecken, D. J., Phillips, S., Sarwar, G., and Jang, C.: Effects of using the CB05 vs. SAPRC99 vs. CB4 chemical mechanism on model predictions: ozone and gas-phase photochemical precursor concentrations, Atmos. Environ., 42, 5805–5820, 2008.
Mao, H. and Talbot, R.: O_3 and CO in New England: temporal variations and relationships, J. Geophys. Res., 109, D21304, doi:10.1029/2004JD004913, 2004.
Mathur, R., Young, J. O., Schere, K. L., and Gipson, L. G.: A comparison of numerical techniques for solution of atmospheric kinetic equations, Atmos. Environ., 32, 1535–1553, 1998.
Mathur, R.: Estimating the impact of the 2004 Alaskan forest fires on episodic particulate matter pollution over the eastern United States through assimilation of satellite derived aerosol optical depth in a regional air quality model, J. Geophys. Res., 113, D17302, doi:10.1029/2007JD009767, 2008.
McRae, G. J., Goodin, W. R., and Seinfeld, J. H.: Numerical solution of atmospheric diffusion equation for chemically reactive flows, J. Comput. Physics., 45, 1–42, 1982.
Pouliot, G. A.: The emissions processing system for the Eta/CMAQ air quality forecast system, Proc. 7th Conf. on Atmospheric Chemistry, The 85th AMS Annual Meeting, Paper 4.5, Amer. Meteor. Soc., San Diego, CA, 2005.
Ridley, B. A., Pickering, K. E., and Dye, J. E.: Comments on the parameterization of lightning-produced NO in global chemistry-transport models, Atmos. Environ., 39, 6184–6187, 2005.
Rogers, E., Black, T., Deaven, D., DiMego, G., Zhao, Q., Baldwin, M., Junker, N., and Lin, Y.: Changes to the operational "early" Eta analysis/forecast system at the National Centers for Environmental Prediction, Weather Forecast., 11, 391–413, 1996.
Russell, A. and Dennis, R.: NARSTO critical review of photochemical models and modeling,

Atmos. Environ., 34, 2283–2324, 2000.
Singh, H. B., Salas, L., Herlth, D., et al.: Reactive nitrogen distribution and partitioning in the North American troposphere and lowermost stratosphere, J. Geophys. Res., 112, D12S04, doi:10.1029/2006JD007664, 2007.
Stockwell, W. R.: A homogeneous gas phase mechanism for use in a regional acid deposition model, Atmos. Environ., 20, 1615–1632, 1986.
Yarwood, G., Rao, S., Yocke, M., and Whitten, G. Z.: Updates to the Carbon Bond chemical mechanism: CB05, Final Report to the US EPA, RT-0400675, 8 December 2005, http://www.camx.com/publ/pdfs/CB05_Final_Report_120805.pdf, 2005.
Yu, S. C., Eder, B., Dennis, R., Chu, S-H., and Schwartz, S.: New unbiased symmetric metrics for evaluation of air quality models, Atmos. Sci. Lett., 7, 26–34, 2006.
Yu, S. C., Mathur, R., Kang, D., Schere, K., Pleim, J., and Otte, T. L.: A detailed evaluation of the Eta-CMAQ forecast model performance for O_3, its related precursors, and meteorological parameters during the 2004 ICARTT study, J. Geophys. Res., 112, D12S14, doi:10.1029/2006JD007715, 2007.

Table 1. Comparison of the reaction rates of inorganic species at 298 K and 1 atm (s^{-1} for first order reactions, cm^3 $molecule^{-1}$ s^{-1} for second-order, cm^6 $molecule^{-2}$ s^{-1} for third-order reactions) in CB4, CB05 and SAPRC-99. Details on reaction rates and species can be found in Gery et al. (1989), Yarwood et al. (2005) and Carter (2000) for CB4, CB05 and SAPRC-99, respectively.

Reaction	CB4	CB05	SAPRC-99	Comments
NO_x and O_3 chemistry				
$NO_2+h\nu \rightarrow NO+O$	Photolysis	Photolysis	Photolysis	
$O_3+h\nu \rightarrow O+O_2$	Photolysis	Photolysis	Photolysis	
$O_3+h\nu \rightarrow OSD+O_2$	Photolysis	Photolysis	Photolysis	
$HONO+h\nu \rightarrow NO+OH$	Photolysis	Photolysis	Photolysis	
$HONO+h\nu \rightarrow NO_2+HO_2$			Photolysis	Not in CB4, CB05
$O+O_2+M \rightarrow O_3+M$	5.57E-34	6.11E-34	5.79E-34	
$O+NO \rightarrow NO_2$	1.66E-12	1.66E-12	2.48E-12	
$O+NO_2 \rightarrow NO+O_2$	9.30E-12	1.02E-11	9.72E-12	
$O+O_3 \rightarrow 2O_2$			7.96E-15	Not in CB4, CB05
$O1D+H_2O \rightarrow 2OH$	2.20E-10	2.20E-10	2.20E-10	
$O1D+M \rightarrow O+M$	2.58E-11	2.96E-11	2.87E-11	
$O_3+OH \rightarrow HO_2+O_2$	6.83E-14	7.25E-14	6.63E-14	
$O_3+HO_2 \rightarrow OH+2O_2$	2.00E-15	1.93E-15		Not in SAPRC-99
$NO+NO+O_2 \rightarrow 2NO_2$	1.95E-38	1.96E-38	1.95E-38	
$NO+NO_2+H_2O \rightarrow 2HONO$	4.40E-40	5.00E-40		Not in SAPRC-99
$NO+O_3 \rightarrow NO_2+O_2$	1.81E-14	1.95E-14	1.81E-14	
$NO+OH+M \rightarrow HONO+M$	6.70E-12	7.41E-12	7.41E-12	
$NO+HO_2 \rightarrow NO_2+OH$	8.28E-12	8.10E-12	8.41E-12	
$NO_2+NO_3 \rightarrow NO+NO_2+O_2$	4.03E-16	6.56E-16	6.56E-16	
$NO_2+HO_2+M \rightarrow HNO_4+M$	1.48E-12	1.38E-12	1.38E-12	
$HONO+OH \rightarrow NO_2+H_2O$	6.60E-12	4.86E-12	6.46E-12	
$HONO+HONO \rightarrow NO+NO_2$	1.00E-20	1.00E-20		Not in SAPRC-99
$HNO_4+M \rightarrow NO_2+HO_2+M$			7.55E-02	Not in CB4, CB05
$HNO_4+OH \rightarrow NO_2+O_2+H_2O$			5.02E-12	Not in CB4, CB05
$SO_2+OH \rightarrow H_2SO_4+HO_2$	8.89E-13	8.89E-13	9.77E-13	
$CO+OH \rightarrow HO_2+CO_2$	2.40E-13	2.41E-13	2.09E-13	
NO_3 and HNO_3 chemistry				
$NO_3+h\nu \rightarrow NO+O_2$		Photolysis	Photolysis	Not in CB4
$NO_3+h\nu \rightarrow NO_2+O$	Photolysis	Photolysis	Photolysis	
$HNO_3+h\nu \rightarrow NO_2+OH$		Photolysis	Photolysis	Not in CB4
$HNO_4+h\nu \rightarrow 0.61HO_2+0.61NO_2+0.39OH+0.39NO_3$			Photolysis	Not in CB4, CB05
$O+NO_2+M \rightarrow NO_3+M$	1.58E-12	3.28E-12	1.82E-12	
$NO_2+O_3 \rightarrow NO_3+O_2$	3.23E-17	3.23E-17	3.52E-17	
$NO_2+OH \rightarrow HNO_3$	1.15E-11	1.05E-11	8.98E-12	
$HNO_3+OH \rightarrow NO_3+H_2O$	1.47E-13	1.54E-13	1.47E-13	
$NO_3+OH \rightarrow NO_2+HO_2$		2.20E-11	2.00E-11	Not in CB4
$NO_3+HO_2 \rightarrow HNO_3+O_2$		3.50E-12		Not in CB4, SAPRC-99
$NO_3+HO_2 \rightarrow 0.8NO_2+0.2HNO_3+0.8OH+O_2$			4.00E-12	Not in CB4, CB05
$NO_3+NO_3 \rightarrow 2NO_2+O_2$		2.28E-16	2.28E-16	Not in CB4
$NO_3+NO \rightarrow 2NO_2$	3.01E-11	2.65E-11	2.60E-11	
$NO_3+NO_2+M \rightarrow N_2O_5+M$	1.26E-12	1.18E-12	1.54E-12	
$N_2O_5 \rightarrow NO_2+NO_3$	4.36E-02	5.28E-02	5.28E-02	
$N_2O_5+H_2O \rightarrow 2HNO_3$	0.00E+00	0.00E+00	0.00E+00	
HO_2 and H_2O_2 chemistry				
$H_2O_2+h\nu \rightarrow 2OH$	Photolysis	Photolysis	Photolysis	
$HO_2+OH \rightarrow H_2O+O_2$		1.11E-10	1.11E-10	Not in CB4
$HO_2+HO_2 \rightarrow H_2O_2$	2.80E-12	2.93E-12	2.87E-12	
$HO_2+HO_2+H_2O \rightarrow H_2O_2+O_2+H_2O$	6.24E-30	6.58E-30	6.46E-30	
$H_2O_2+OH \rightarrow HO_2+H_2O$	1.66E-12	1.70E-12	1.70E-12	
$OH+H_2 \rightarrow HO_2$		6.69E-15	6.70E-15	Not in CB4

ACPD
9, 22955–22992, 2009

Table 2. The same as Table 1 but for selected organic species (formaldehyde, alkene, isoprene and terpenes, also see Table 3 for the remaining organic species).

Reactions	CB4	CB05	SAPRC-99	Comments
Formaldehyde				
$HCHO+OH \rightarrow HO_2+CO$	1.00E-11	9.00E-12	9.20E-12	Formaldehyde
$HCHO \rightarrow 2HO_2+CO$	Photolysis	Photolysis	Photolysis	
$HCHO \rightarrow CO$	Photolysis	Photolysis	Photolysis	
$HCHO+O \rightarrow OH+HO_2+CO$	1.65E-13	1.58E-13		
$HCHO+NO_3 \rightarrow HNO_3+HO_2+CO$	6.30E-16	5.80E-16	5.73E-16	
$HCHO+HO_2 \rightarrow HCO_3$		7.90E-14	7.90E-14	
$HCO_3 \rightarrow HCHO+HO_2$		1.51E+02	1.51E+02	
$HCO_3+NO \rightarrow HCOOH+NO_2+HO_2$		5.60E-12	7.29E-12	
$HCO_3+HO_2 \rightarrow MEPX$		1.26E-11		
$HCOOH+OH \rightarrow HO_2$		4.00E-13	4.50E-13	Formic acid
$MEO2+NO \rightarrow HCHO+HO_2+NO_2$		7.66E-12	7.29E-12	Methylperoxy radical
$MEO2+HO_2 \rightarrow MEPX$		5.08E-12	5.21E-12	
$MEO2+MEO2 \rightarrow 1.37HCHO+0.74HO_2+0.63MEOH$		3.52E-13		
$MEOH+OH \rightarrow HCHO+HO_2$		9.12E-13	9.14E-13	Methanol
$MEPX \rightarrow HCHO+HO_2+OH$		Photolysis	Photolysis	Methylhydroperoxide
$MEPX+OH \rightarrow 0.7MEO2+0.3XO_2+0.3HO_2$		7.43E-12		
$MEO2+MEO2 \rightarrow MEOH+HCHO$			2.65E-13	Methylperoxy radical
$MEO2+MEO2 \rightarrow 2HCHO+2HO_2$			1.07E-13	
$MEO2+NO_3 \rightarrow HCHO+HO_2+NO_2$			1.30E-12	
$MEPX+HO \rightarrow 0.35HCHO+0.35HO+0.65MEO2$			5.49E-12	Methylhydroperoxide
Alkene reactions				
$OLE+O \rightarrow 0.63ALD2+0.38HO_2+0.28XO_2+0.3CO+0.2HCHO+0.02XO_2N+0.22PAR+0.2OH$	4.05E-12			Terminal Olefin
$OLE+O \rightarrow 0.2ALD2+0.3ALDX+0.3HO_2+0.2XO_2+0.2CO+0.2HCHO+0.01XO_2N+0.2PAR+0.1OH$		3.91E-12		
$OLE+OH \rightarrow HCHO+ALD2+XO_2+HO_2-PAR$	2.82E-11			
$OLE+OH \rightarrow 0.8HCHO+0.33ALD2+0.62ALDX+0.8XO_2+0.95HO_2-0.7PAR$		3.20E-11		
$OLE+O_3 \rightarrow 0.5ALD2+0.74HCHO+0.33CO+0.44HO_2+0.22XO_2+0.1OH+0.2HCOOH+0.2AACD-PAR$	1.20E-17			
$OLE+O_3 \rightarrow 0.18ALD2+0.74HCHO+0.32ALDX+0.22XO_2+0.1OH+0.33CO+0.44HO_2-1.0PAR$		1.11E-17		
$OLE+NO_3 \rightarrow 0.91XO_2+0.09XO_2N+HCHO+ALD2-PAR+NO_2$	7.70E-15			
$NO_3+OLE \rightarrow NO_2+HCHO+0.91XO_2+0.09XO_2N+0.56ALDX+0.35ALD2-1PAR$		4.98E-16		
$OLE1+HO \rightarrow 0.91RO2\_R+0.09RO2\_N+0.205R2O2+0.732HCHO+0.294ALD2+0.497RCHO+0.005ACET+0.119PROD2$			3.23E-11	Alkene 1
$OLE1+O_3 \rightarrow 0.155HO+0.056HO_2+0.022RO2\_R+0.001RO2\_N+0.076MEO2+0.345CO+0.5HCHO+0.154ALD2+0.363RCHO+0.001ACET+0.215PROD2+0.185HCOOH+0.05CCO\_OH+0.119RCO\_OH$			1.07E-17	
$OLE1+NO_3 \rightarrow 0.824RO2\_R+0.176RO2\_N+0.488R2O2+0.009ALD2+0.037RCHO+0.024ACET+0.511NTR$			1.26E-14	
$OLE1+O \rightarrow 0.45RCHO+0.437MEK+0.113PROD2$			4.88E-12	
$OLE2+HO \rightarrow 0.918RO2\_R+0.082RO2\_N+0.001R2O2+0.244HCHO+0.732ALD2+0.511RCHO+0.127ACET+0.072MEK+0.061BALD+0.025METHACRO+0.025ISOPROD+OLE2AER$			6.31E-11	Alkene 2
$OLE2+O_3 \rightarrow 0.378HO+0.003HO_2+0.033RO2\_R+0.002RO2\_N+0.137R2O2+0.197MEO2+0.137C2O3+0.006RCO\_O2+0.265CO+0.269HCHO+0.456ALD2+0.305RCHO+0.045ACET+0.026MEK+0.006PROD2+0.042BALD+0.026METHACRO+0.073HCOOH+0.129CCO\_OH+0.303RCO\_OH+OLE2AER$			1.07E-16	

ACPD

9, 22955–22992, 2009

Table 2. Continued.

Reactions	CB4	CB05	SAPRC-99	Comments
OLE2+NO_3→0.391NO2+0.442RO2_R+0.136RO2_N+0.711R2O2+ 0.03MEO2+0.079HCHO+0.507ALD2+0.151RCHO+0.102ACET+ 0.001MEK+0.015BALD+0.048MVK+0.321NTR+OLE2AER			7.26E-13	
OLE2+O→0.013HO_2+0.012RO2_R+0.001RO2_N+0.012CO+ 0.069RCHO+0.659MEK+0.259PROD2+0.012METHACRO			2.09E-11	
ETH+O→HCHO+0.7XO_2+CO+1.7HO_2+0.3OH	7.01E-13	7.29E-13		Ethene
ETH+O→0.5HO_2+0.2RO2_R+0.3MEO2+0.491CO+0.191HCHO+ 0.25ALD2+0.009GLY			7.29E-13	
ETH+OH→XO_2+1.56HCHO+HO_2+0.22ALD2	7.94E-12	8.15E-12		
ETH+OH→RO2_R+1.61HCHO+0.195ALD2			8.52E-12	
ETH+O_3→HCHO+0.42CO+0.12HO_2+0.4HCOOH	1.89E-18			
ETH+O_3→HCHO+0.63CO+0.13HO_2+0.13OH+0.37HCOOH		1.76E-18		
ETH+O_3→0.12HO+0.12HO_2+0.5CO+HCHO+0.37HCOOH			1.59E-18	
ETH+NO_3→NO_2+XO_2+2HCHO		2.10E-16		
ETH+NO_3→RO2_R+RCHO			2.05E-16	
IOLE+O→1.24ALD2+0.66ALDX+0.1HO_2+0.1XO_2+0.1CO+0.1PAR		2.30E-11		Internal olefin
IOLE+OH→1.300ALD2+0.700ALDX+HO_2+XO2		6.33E-11		
IOLE+O_3→0.65ALD2+0.35ALDX+0.25HCHO+0.25CO+0.5O+0.5OH+ 0.5HO_2		2.09E-16		
IOLE+NO_3→1.180ALD2+0.640ALDX+HO_2+NO_2		3.88E-13		
METHACRO+HO→0.5RO2_R+0.416CO+0.084HCHO+0.416MEK+ 0.084MGLY+0.5MA_RCO3			3.36E-11	Methacrolein
METHACRO+O_3→0.008HO_2+0.1RO2_R+0.208HO+0.1RCO_O2+ 0.45CO+0.2HCHO+0.9MGLY+0.333HCOOH			1.13E-18	
METHACRO+NO_3→0.5HNO_3+0.5RO2_R+0.5CO+0.5MA_RCO3			4.58E-15	
METHACRO+O3P→RCHO			6.34E-12	
METHACRO→0.34HO_2+0.33RO2_R+0.33HO+0.67C2O3+0.67CO+ 0.67HCHO+0.33MA_RCO3			Photolysis	
MA_RCO3+NO_2→MA_PAN			1.21E-11	Peroxyacyl radicals from methacrolein
MA_RCO3+NO→NO_2+HCHO+C_2O_3			2.80E-11	
MA_RCO3+HO_2→0.75RCO_OOH+0.25RCO_OH+0.25O3			1.41E-11	
MA_RCO3+NO_3→NO_2+HCHO+C_2O_3			4.00E-12	
MA_RCO3+MEO2→RCO_OH+HCHO			9.64E-12	
MA_RCO3+RO2_R→RCO_OH			7.50E-12	
MA_RCO3+R2O2→MA_RCO3			7.50E-12	
MA_RCO3+RO2_N→2RCO_OH			7.50E-12	
MA_RCO3+C_2O_3→MEO2+HCHO+C_2O_3			1.55E-11	
MA_RCO3+RCO_O2→HCHO+C_2O_3+ALD2+RO2_R			1.55E-11	
MA_RCO3+BZCO_O2→HCHO+C_2O_3+BZ_O+R2O2			1.55E-11	
MA_RCO3+MA_RCO3→2HCHO+2C2O3			1.55E-11	
Isoprene reactions				
ISOP+O→0.75ISPD+0.50HCHO+0.25XO_2+0.25HO_2+0.25C2O3+ 0.25PAR	3.60E-11	3.60E-11		Isoprene
ISOP+O→0.01RO2_N+0.24R2O2+0.25MEO2+0.24MA_RCO3+ 0.24HCHO+0.75PROD2			3.60E-11	
ISOP+OH→0.912ISPD+0.629HCHO+0.991XO_2+0.912HO_2+ 0.088XO2N	9.97E-11	9.97E-11		
ISOP+HO→0.907RO2_R+0.093RO2_N+0.079R2O2+0.624HCHO+ 0.23METHACRO+0.32MVK+0.357ISOPROD			9.83E-11	
ISOP+O_3→0.65ISPD+0.60HCHO+0.20XO_2+0.066HO_2+0.266OH+ 0.20C2O3+0.15ALD2+0.35PAR+0.066CO	1.29E-17	1.29E-17		
ISOP+O_3→0.266HO+0.066RO2_R+0.008RO2_N+0.126R2O2+ 0.23METHACRO+0.192MA_RCO3+0.275CO+0.592HCHO+ 0.1PROD2+0.39METHACRO+0.15RCO_OH			1.29E-17	

ACPD

9, 22955–22992, 2009

Table 2. Continued.

Reactions	CB4	CB05	SAPRC-99	Comments
ISOP+NO_3→0.2ISPD+0.8NTR+1XO_2+0.8HO_2+0.2NO2+ 0.8ALD2+2.4PAR	6.74E-13	6.74E-13	6.74E-13	
ISOP+NO_2→0.2ISPD+0.8NTR+1XO_2+0.8HO_2+0.2NO+ 0.8ALD2+2.4PAR	1.49E-19	1.50E-19		
ISPD+OH→1.565PAR+0.167HCHO+0.713XO_2+0.503HO_2+ 0.334CO+0.168MGLY+0.273ALD2+0.498C2O3	3.36E-11			Isoprene product
ISPD+OH→1.565PAR+0.167HCHO+0.713XO_2+0.503HO_2+ 0.334CO+0.168MGLY+0.252ALD2+0.21C2O3+0.25CXO3+ 0.12ALDX		3.36E-11		
ISPD+OH→0.67RO2_R+0.041RO2_N+0.289MA_RCO3+ 0.336CO+0.055HCHO+0.129ALD2+0.013RCHO+0.15MEK+ 0.332PROD2+0.15GLY+0.174MGLY			6.19E-11	
ISPD+O_3→0.114C2O3+0.15HCHO+0.85MGLY+0.154HO_2+ 0.268OH+0.064XO_2+0.02ALD2+0.36PAR+0.225CO	7.11E-18	7.10E-18		
ISPD+O_3→0.4HO_2+0.048RO2_R+0.048RCO_O2+0.285HO+ 0.498CO+0.125HCHO+0.047ALD2+0.21MEK+0.023GLY+ 0.742MGLY+0.1HCOOH+0.372RCO_OH			4.18E-18	
ISPD+NO_3→0.357ALD2+0.282HCHO+1.282PAR+0.925HO_2+ 0.643CO+0.850NTR+0.075C2O3+0.075XO_2+0.075HNO_3	1.00E-15			
ISPD+NO_3→0.357ALDX+0.282HCHO+1.282PAR+0.925HO_2+ 0.643CO+0.85NTR+0.075CXO3+0.075XO_2+0.15HNO_3		1.00E-15		
ISPD+NO_3→0.799RO2_R+0.051RO2_N+0.15MA_RCO3+0.572CO+ 0.15HNO_3+0.227HCHO+0.218RCHO+0.008MGLY+0.572NTR			1.00E-13	
ISPD→0.333CO+0.067ALD2+0.900HCHO+0.832PAR+1.033HO_2+ 0.700XO_2+0.967C2O3	Photolysis	Photolysis		
ISPD→1.233HO_2+0.467C2O3+0.3RCO_O2+1.233CO+0.3HCHO+ 0.467ALD2+0.233MEK			Photolysis	
Terpene reactions				
TERP+O→0.150ALDX+5.12PAR+TERPAER		3.60E-11		Terpenes
TRP1+O→0.147RCHO+0.853PROD2+TRP1AER			3.27E-11	Terpenes
TERP+OH→TERPAER+OH	8.26E-11			
TERP+OH→0.750HO_2+1.250XO_2+0.250XO_2N+ 0.280HCHO+1.66 PAR+0.470ALDX+TERPAER		6.77E-11	8.26E-11	
TERP+NO_3→TERPAER+NO3	6.58E-12			
TERP+NO_3→0.47NO2+0.28HO_2+1.03XO_2+0.25XO_2N+ 0.47ALDX+0.53NTR+TERPAER		6.66E-12		
TRP1+NO_3→0.474NO2+0.276RO2_R+0.25RO2_N+0.75R2O2+ 0.474RCHO+0.276NTR+TRP1AER			6.58E-12	
TERP+O_3→TERPAER+O_3	6.87E-17			
TERP+O_3→0.57OH+0.07HO_2+0.76XO_2+0.18XO_2N+ 0.24HCHO+0.001CO+7PAR+0.21ALDX+0.39CXO3+TERPAER		7.63E-17		
TRP1+O_2→0.567HO+0.033HO_2+0.031RO2_R+0.18RO2_N+ 0.729R2O2+0.123C2O3+0.201RCO_O2+0.157CO+0.235HCHO+ 0.205RCHO+0.13ACET+0.276PROD2+0.001GLY+0.031BACL+ 0.103HCOOH+0.189RCO_OH+TRP1AER			6.87E-17	

ACPD
9, 22955–22992, 2009

Table 3. Comparison of observations and models (CB4, CB05 and SAPRC-99) for different gaseous species (O_3, CO, PAN, NO_x, NO, NO_2, HNO_3, NO_y, ethylene, NO_z, and NO_2+O_3 on the basis of all P-3 and DC-8 aircraft measurements during the 2004 ICARTT (mean±standard deviation, all units are ppbv except that PAN, isoprene, and terpenes units are pptv).

	Mean±standard deviation				NMB (%)		
	Obs	CB4	CB05	SAPRC-99	CB4	CB05	SAPRC-99
P3							
O_3	55.4±16.2	61.3±16.1	67.1±17.4	68.9±18.0	10.8	21.1	24.3
O_3+NO_2	58.5±14.9	63.4±16.5	69.6±17.4	71.3±17.8	8.3	19.0	22.0
NO_z	2.7±1.4	5.4±2.4	5.5±2.5	4.3±2.1	101.2	108.0	63.1
PAN	348.1±176.7	1047.8±525.0	1054.0±544.1	768.9±445.0	201.0	202.8	120.9
NO_y	4.1±2.5	6.3±3.1	6.4±3.1	5.3±2.8	53.0	55.8	28.3
CO	139.3±36.0	124.8±33.2	129.6±33.2	121.2±35.5	−10.4	−6.9	−13.0
HNO_3	1.8±1.8	1.6±1.6	1.4±1.4	1.5±1.5	−8.9	−19.9	−16.1
NO_2	0.8±1.4	0.6±0.9	0.8±1.2	0.7±0.9	−22.5	−2.4	−19.3
NO	0.2±0.8	0.1±0.2	0.1±0.2	0.1±0.2	−56.2	−61.0	−56.8
NO_x	1.0±2.1	0.7±1.0	0.8±1.2	0.7±1.0	−32.8	−17.9	−30.4
SO_2	1.7±2.7	1.5±2.0	1.6±2.0	1.7±2.0	−9.7	−2.9	−1.4
Isoprene	69.7±100.4	65.5±140.9	73.5±145.7	63.8±138.5	−6.0	5.5	−8.4
Terpenes	15.6±12.4	4.3±11.1	5.1±11.5	3.9±9.9	−72.2	−67.3	−74.9
DC-8							
O_3	57.5±19.9	68.6±37.5	72.0±36.3	73.8±37.1	19.2	25.2	28.4
HNO_3	0.8±0.8	0.9±0.9	0.8±0.8	0.9±0.9	13.5	0.7	4.7
HCHO	0.9±0.6	1.6±1.1	1.2±0.8	1.1±0.8	82.1	39.0	26.2
H_2O_2	2.1±1.0	3.7±1.6	2.4±1.0	1.6±0.8	74.7	10.8	−25.5
CO	130.2±35.4	99.6±22.3	101.8±23.4	93.2±24.4	−23.5	−21.8	−28.4
NO_2	0.5±1.3	0.3±0.8	0.3±0.7	0.4±0.7	−33.9	−35.0	−30.5
SO_2	1.1±1.5	0.8±1.1	0.8±1.1	0.8±1.1	−26.1	−20.4	−21.5
NO	0.2±0.3	0.1±0.2	0.1±0.2	0.1±0.2	−58.6	−60.7	−55.3

ACPD
9, 22955–22992, 2009

Table 4. Comparison of observations and models (CB4, CB05 and SAPRC-99) for different gaseous species (O_3, CO, PAN, NO, NO_2, NO_y, SO_2 and NO_2+O_3 along the ship tracks for different offshore flows during the 2004 ICARTT (mean±standard deviation, all units are ppbv except that isoprene unit is pptv). Correlations between O_3 and NO_z for the NO_x limited conditions indicated by the observational data with $[O_3]/[NO_x]>46$ (aged air masses) (see text for explanation).

	Mean±standard deviation				NMB (%)		
	Obs	CB4	CB05	SAPRC-99	CB4	CB05	SAPRC-99
Southwest/west offshore flows							
O_3	44.6±18.9	56.9±23.0	62.7±25.2	65.6±27.6	27.6	40.6	47.1
O_3+NO_2	48.1±17.6	60.5±19.5	66.0±22.1	69.0±24.7	25.6	37.1	43.4
Isoprene	135.8±164.3	41.4±82.2	42.1±84.4	39.8±82.8	−69.5	−69.0	−70.7
CO	190.4±63.3	197.1±100.9	190.2±90.8	179.9±89.1	3.5	−0.1	−5.5
NO_y	6.7±7.4	10.6±10.8	10.2±10.0	8.8±9.8	58.1	52.6	31.8
NO_2	3.5±4.5	3.6±7.4	3.4±6.9	3.5±7.0	5.3	−2.6	1.4
NO	1.0±2.5	1.1±4.5	0.8±3.9	0.8±3.9	9.7	−16.0	−15.4
PAN	0.7±0.6	1.1±0.7	1.2±0.8	0.8±0.6	60.4	72.4	24.3
SO_2	1.1±1.2	2.1±2.2	2.3±2.1	2.3±2.1	97.5	113.3	117.1
East/north/northwest/south clean marine or continental flows							
O_3	35.0±12.5	37.2±10.2	39.7±10.0	41.2±9.9	6.2	13.6	17.7
O_3+NO_2	36.8±12.2	37.8±10.3	40.4±10.2	41.8±10.1	3.0	9.9	14.0
Isoprene	81.3±95.8	71.4±141.1	81.7±148.6	78.8±151.9	−12.2	0.5	−3.0
CO	146.5±21.1	104.5±15.4	101.0±14.1	87.5±18.6	−28.6	−31.1	−40.3
NO_y	3.3±4.6	2.3±1.1	2.0±0.9	1.3±0.8	−31.3	−41.8	−62.6
NO_2	1.6±2.0	0.6±0.8	0.4±0.6	0.5±0.6	−63.6	−72.5	−70.8
NO	1.5±10.8	0.03±0.07	0.02±0.05	0.02±0.05	−97.8	−98.5	−98.3
PAN	0.8±0.5	0.7±0.4	0.4±0.2	0.3±0.2	−11.7	−48.9	−65.6
SO_2	0.6±0.9	0.39±0.39	0.37±0.36	0.38±0.37	−36.0	−38.8	−36.7

All data

Obs (n=138):	$[O_3]$=11.8$[NO_z]$+36.8, r=0.591
CB4 (n=138):	$[O_3]$= 4.0$[NO_z]$+38.3, r=0.805
CB05 (n=138):	$[O_3]$= 4.5$[NO_z]$+42.1, r=0.798
SAPRC-99 (n=138):	$[O_3]$= 5.8$[NO_z]$+45.8, r=0.786

ACPD
9, 22955–22992, 2009

Table 5. Comparison of observations and models (CB4, CB05 and SAPRC-99) for different gaseous species (O_3, CO, NO, NO_y, SO_2) at four AIRMAP sites during the 2004 ICARTT (mean±standard deviation, all units are ppbv).

	Mean±standard deviation				NMB (%)		
	Obs	CB4	CB05	SAPRC-99	CB4	CB05	SAPRC-99
Castle Springs (*n*=842)							
NO	0.14±0.2	0.05±0.07	0.04±0.05	0.04±0.05	−66.9	−73.7	−69.2
NO_Y	2.2±1.5	3.4±2.5	3.1±2.4	2.4±2.0	55.9	41.9	9.8
O_3	35.2±13.0	46.8±15.0	51.9±16.1	52.7±16.8	33.2	47.5	50.0
CO	189.8±45.5	112.1±31.2	113.1±31.5	105.0±32.7	−40.9	−40.4	−44.7
SO_2	1.3±2.3	1.0±1.4	1.2±1.7	1.1±1.7	−21.2	−7.3	−13.2
Isle of Schoals (*n*=864)							
O_3	36.8±17.1	52.4±16.9	57.7±19.8	58.9±21.9	42.2	56.6	59.9
CO	175.2±52.9	124.1±44.0	124.2±42.2	112.6±44.4	−29.1	−29.1	−35.7
NO	0.8±1.4	0.2±1.1	0.07±0.33	0.09±0.40	−74.5	−90.8	−88.1
Mount Washington (*n*=864)							
O_3	46.6±12.7	49.3±14.3	53.3±15.5	54.7±16.8	5.7	14.3	17.4
NO	4.3±15.5	0.01±0.01	0.01±0.01	0.01±0.03	−99.7	−99.7	−99.6
CO	157.5±45.8	96.2±19.8	98.5±20.9	91.1±23.8	−38.9	−37.4	−42.2
NO_Y	4.4±13.5	2.4±1.7	2.2±1.6	1.7±1.3	−44.4	−50.0	−61.0
SO_2	0.9±1.6	0.4±0.5	0.5±0.7	0.5±0.7	−55.2	−44.8	−39.2
Thompson Farm (*n*=864)							
O_3	28.2±18.7	43.9±17.7	49.7±18.2	51.4±19.5	55.3	76.1	82.0
NO	0.3±0.7	0.2±0.4	0.2±0.2	0.2±0.3	−28.6	−48.2	−47.5
CO	173.4±48.6	160.8±57.9	154.1±50.5	150.0±57.1	−7.3	−11.1	−13.6
NO_Y	3.9±2.6	7.4±4.8	6.5±4.2	6.1±4.1	89.2	65.3	55.2
SO_2	1.1±2.4	1.5±1.2	1.7±1.3	1.7±1.3	32.0	49.1	54.1

ACPD
9, 22955–22992, 2009

Table 6. The Same as Table 2 but for remaining organic reactions for Table 2.

Reactions	CB4	CB05	SAPRC-99	Comments
Higher molecular weight Aldehyde				
ALD2+O→C2O3+OH	4.39E-13	4.49E-13		Acetaldehyde
ALD2+OH→C2O3	1.62E-11	1.39E-11	1.58E-11	
ALD2+NO_3→C2O3+HNO_3	2.50E-15	2.38E-15	2.73E-15	
ALD2→MEO2+CO+HO_2		Photolysis	Photolysis	
ALD2→XO_2+2HO_2+CO+HCHO	Photolysis			
C2O3+NO→NO_2+XO_2+HCHO+HO_2	1.91E-11	2.00E-11	2.13E-11	Acetylperoxy radical
C2O3+NO_2→PAN	9.41E-12	1.05E-11	1.05E-11	
C2O3+C2O3→2XO_2+2HCHO+2HO_2	2.50E-12		1.55E-11	
C2O3+C2O3→2MEO2		1.55E-11		
C2O3+HO_2→0.79HCHO+0.79XO_2+0.79HO_2+0.79OH+0.21PACD	6.50E-12			
C2O3+HO_2→0.8PACD+0.2AACD+0.2O_3		1.41E-11		
C2O3+MEO2→0.9MEO2+0.9HO_2+HCHO+0.1AACD		1.07E-11		
C2O3+XO_2→0.9MEO2+0.1AACD		1.60E-11		
C2O3+MEO2→CCO_OH+HCHO			9.64E-12	
C2O3+HO_2→0.75CCO_OOH+0.25CCO_OH+0.25O_3			1.41E-11	
C2O3+NO_3→MEO2+NO_2			4.00E-12	
C2O3+RO2_R→CCO_OH			7.50E-12	
C2O3+R2O2→C2O3			7.50E-12	
C2O3+RO2_N→CCO_OH+PROD2			7.50E-12	
PAN→C2O3+NO_2	4.23E-04	3.31E-04	5.21E-04	Peroxyl acyl nitrate
PAN→C2O3+NO_2		Photolysis		
PAN2→RCO_O2+NO_2			4.43E-04	PPN and other higher alky PAN analogues
MA_PAN→MA_RCO3+NO_2			3.55E-04	
PACD+OH→C2O3		7.83E-13		Peroxycarboxylic acid
PACD→MEO2+OH		Photolysis		
AACD+OH→MEO2		7.83E-13		Carboxylic acid
ALDX+O→CXO3+OH		7.02E-13		Propionaldehyde and higher aldehydes
ALDX+OH→CXO3		1.99E-11		
ALDX+NO_3→CXO3+HNO_3		6.50E-15		
ALDX→MEO2+CO+HO_2		Photolysis		
CXO3+NO→ALD2+NO_2+HO_2+XO_2		2.10E-11		C_3 and higher acylperoxy radical
CXO3+NO_2→PANX		1.05E-11		
CXO3+HO_2→0.8PACD+0.2AACD+0.2O_3		1.41E-11		
CXO3+MEO2→0.9ALD2+0.9XO_2+HO_2+0.1AACD+0.1HCHO		1.07E-11		
CXO3+XO_2→0.9ALD2+0.1AACD		1.60E-11		
CXO3+CXO3→2ALD2+2XO_2+2HO_2		1.55E-11		
CXO3+C2O3→MEO2+XO_2+HO_2+ALD2		1.55E-11		
PANX→CXO3+NO_2		3.31E-04		C_3 and higher peroxyacyl nitrates
PANX→CXO3+NO_2		Photolysis		
PANX+OH→ALD2+NO_2		3.00E-13		
NTR+OH→HNO_3+HO_2+0.33HCHO+0.33ALD2+0.33ALDX−0.66PAR		1.76E-13		Organic nitrate (RNO_3)
NTR→NO_2+HO_2+0.33HCHO+0.33ALD2+0.33ALDX−0.66PAR		Photolysis		
NTR+HO→0.338NO2+0.113HO_2+0.376RO2_R+0.173RO2_N+0.596R2O2+0.01HCHO+0.439ALD2+0.213RCHO+0.006ACET+0.177MEK+ 0.048PROD2+0.31NTR			7.80E-12	
NTR→NO_2+0.341HO_2+0.564RO2_R+0.095RO2_N+0.152R2O2+0.134HCHO+0.431ALD2+0.147RCHO+0.02ACET+0.243MEK+0.435PROD2			Photolysis	
ROOH+OH→XO_2+0.5ALD2+0.5ALDX		5.69E-12		Higher organic peroxide
ROOH+HO→RCHO+0.34RO2_R+0.66HO			1.10E-11	
ROOH→OH+HO_2+0.5ALD2+0.5ALDX		Photolysis		

ACPD

9, 22955–22992, 2009

Table 6. Continued.

Reactions	CB4	CB05	SAPRC-99	Comments
ETOH+OH→HO_2+0.9ALD2+0.05ALDX+0.1HCHO+0.1XO_2		3.19E-12		Ethanol
ROOH→RCHO+HO_2+HO			Photolysis	Lumped C3+ aldehydes
RCHO+HO→0.034RO2_R+0.001RO2_N+0.965RCO_O2+ 0.034CO+0.034ALD2			2.00E-11	
RCHO+NO_3→HNO_3+RCO_O2			3.67E-15	
RCHO→ALD2+RO2_R+CO+HO_2			Photolysis	
CCO_OH+HO→0.13RO2_R+0.87MEO2+0.13MGLY			8.00E-13	Peroxy acetic acid
RCO_OH+HO→RO2_R+0.605ALD2+0.21RCHO+0.185BACL			1.16E-12	Higher organic acids
Alkane reactions				
CH_4+OH→XO_2+HCHO+HO_2	7.73E-15			Methane
CH_4+OH→MEO2		6.34E-15	6.37E-15	
ETHA+OH→0.991ALD2+0.991XO_2+0.009XO_2N+HO_2		2.40E-13		Ethane
PAR+OH→0.87XO_2+0.13XO_2N+0.11HO_2+0.11ALD2+0.76ROR− 0.11PAR	8.10E-13			Paraffin carbon bond
PAR+OH→0.87XO_2+0.13XO_2N+0.11HO_2+0.06ALD2−0.11PAR+ 0.76ROR+0.05ALDX		8.10E-13		
ROR→1.1ALD2+0.96XO_2+0.94HO_2−2.10PAR+0.04XO_2N+0.02ROR	2.19E+03			Secondary alkoxy radical
ROR→0.96XO_2+0.6ALD2+0.94HO_2−2.1PAR+0.04XO_2N+ 0.02ROR+0.5ALDX		2.19E+03		
ROR→HO_2	1.60E+03	1.60E+03		
ROR+NO_2→NTR	1.50E-11	1.50E-11		
ALK1+HO→RO2_R+ALD2			2.54E-13	Alkane 1
ALK2+HO→0.246HO+0.121HO_2+0.612RO2_R+0.021RO2_N+ 0.16CO+0.039HCHO+0.155RCHO+0.417ACET+0.248GLY+ 0.121HCOOH			1.04E-12	Alkane 2
ALK3+HO→0.695RO2_R+0.07RO2_N+0.559R2O2+0.236TBU_O+ 0.026HCHO+0.445ALD2+0.122RCHO+0.024ACET+0.332MEK			2.38E-12	Alkane 3
ALK4+HO→0.835RO2_R+0.143RO2_N+0.936R2O2+0.011MEO2+ 0.011C2O3+0.002CO+0.024HCHO+0.455ALD2+0.244RCHO+ 0.452ACET+0.11MEK+0.125PROD2			4.38E-12	Alkane 4
ALK5+HO→0.653RO2_R+0.347RO2_N+0.948R2O2+0.026HCHO+ 0.099ALD2+0.204RCHO+0.072ACET+0.089MEK+0.417PROD2+ ALK5AER			9.32E-12	Alkane 5
Aromatic reactions				
TOL+OH→0.08XO_2+0.36CRES+0.44HO_2+0.56TO2+TOLAER	6.19E-12	5.92E-12		Toluene
ARO1+OH→0.224HO_2+0.765RO2_R+0.011RO2_N+0.055PROD2+ 0.118GLY+0.119MGLY+0.017PHEN+0.207CRES+0.059BALD+ 0.491DCB1+0.108DCB2+0.051DCB3+ARO1AER			5.96E-12	Aromatic 1
TO2+NO→0.9NO2+0.9HO_2+0.9OPEN +0.1NTR	8.10E-12	8.10E-12		Toluene-hydroxyl radical adduct
TO2→CRES+HO_2	4.20E+00	4.20E+00		
ARO2+HO→0.187HO_2+0.804RO2_R+0.009RO2_N+0.097GLY+ 0.287MGLY+0.087BACL+0.187CRES+0.05BALD+0.561DCB1+ 0.099DCB2+0.093DCB3+ARO2AER			2.64E-11	Aromatic 2
CRES+OH→0.4CRO+0.6XO_2+0.6HO_2+0.3OPEN+CSLAER	4.10E-11	4.10E-11		Cresols
CRES+OH→0.24BZ_O+0.76RO2_R+0.23MGLY+CRESAER			4.20E-11	
CRES+NO_3→CRO+HNO_3+CSLAER	2.20E-11	2.20E-11		
CRES+NO_3→HNO_3+BZ_O+CRESAER			1.37E-11	
CRO+NO_2→NTR	1.40E-11	1.40E-11		
CRO+HO_2→CRES		5.50E-12		Methylphenoxy radical
XYL+OH→0.7HO_2+0.5XO_2+0.2CRES+0.8MGLY+1.1PAR+ 0.3TO2+XYLAER	2.51E-11	2.51E-11		Xylene

ACPD

9, 22955–22992, 2009

Table 6. Continued.

Reactions	CB4	CB05	SAPRC-99	Comments
OPEN+OH→XO_2+2CO+2HO_2+C2O3+HCHO	3.00E-11	3.00E-11		Aromatic ring opening product
OPEN→C2O3+HO_2+CO	Photolysis	Photolysis		
OPEN+O_3→0.03ALD2+0.62C2O3+0.7HCHO+0.03XO_2+ 0.69CO+0.08OH+0.76HO_2+0.2MGLY	1.01E-17	1.01E-17		
MGLY+OH→XO_2+C2O3	1.70E-11	1.80E-11		Methylglyoxal
MGLY+HO→CO+C2O3			1.50E-11	
MGLY→C2O3+HO_2+CO	Photolysis	Photolysis	Photolysis	
MGLY+NO_3→HNO_3+CO+C2O3			2.42E-15	Glyoxal
GLY→2CO+2HO_2			Photolysis	
GLY→HCHO+CO			Photolysis	
GLY+HO→0.63HO_2+1.26CO+0.37RCO_O2			1.10E-11	
GLY+NO_3→HNO_3+0.63HO_2+1.26CO+0.37RCO_O2			9.65E-16	
DCB1+HO→RCHO+RO2_R+CO			5.00E-11	Reactive aromatic fragmentation product 1
DCB1+O_3→1.5HO_2+0.5HO+1.5CO+GLY			2.00E-18	
DCB2+HO→R2O2+RCHO+C2O3			5.00E-11	Reactive aromatic fragmentation product 2
DCB2→RO2_R+0.5C2O3+0.5HO_2+CO+R2O2+0.5GLY+0.5MGLY			Photolysis	
DCB3+HO→R2O2+RCHO+C2O3			5.00E-11	Reactive aromatic fragmentation product 3
DCB3→RO2_R+0.5C2O3+0.5HO_2+CO+R2O2+0.5GLY+0.5MGLY			Photolysis	
PHEN+HO→0.24BZ_O+0.76RO2_R+0.23GLY			2.63E-11	Phenol
PHEN+NO_3→HNO_3+BZ_O			3.78E-12	
Ketone				
ACET+HO→HCHO+C2O3+R2O2			1.92E-13	Acetone
ACET→C2O3+MEO2			Photolysis	
MEK+HO→0.37RO2_R+0.042RO2_N+0.616R2O2+0.492C2O3+ 0.096RCO_O2+0.115HCHO+0.482ALD2+0.37RCHO			1.18E-12	Ketones
MEK→C2O3+ALD2+RO2_R			Photolysis	
MVK+HO→0.3RO2_R+0.025RO2_N+0.675R2O2+0.675C2O3+ 0.3HCHO+0.675RCHO+0.3MGLY			1.89E-11	Methyl vinyl ketones
MVK+O_3→0.064HO_2+0.05RO2_R+0.164HO+0.05RCO_O2+ 0.475CO+0.1HCHO+0.95MGLY+0.351HCOOH			4.58E-18	
MVK+O3P→0.45RCHO+0.55MEK			4.32E-12	
MVK→0.3MEO2+0.7CO+0.7PROD2+0.3MA_RCO3			Photolysis	
PROD2+HO→0.379HO_2+0.473RO2_R+0.07RO2_N+0.029C2O3+ 0.049RCO_O2+0.213HCHO+0.084ALD2+0.558RCHO+ 0.115MEK+0.329PROD2			1.50E-11	
PROD2→0.96RO2_R+0.04RO2_N+0.515R2O2+0.667C2O3+ 0.333RCO_O2+0.506HCHO+0.246ALD2+0.71RCHO			Photolysis	
other				
RO2_R+NO→NO_2+HO_2			9.04E-12	Peroxy radical operator
RO2_R+HO_2→ROOH			1.49E-11	
RO2_R+NO_3→NO_2+HO_2			2.30E-12	
RO2_R+MEO2→HO_2+0.75HCHO+0.25MEOH			2.00E-13	
RO2_R+RO2_R→HO_2			3.50E-14	
R2O2+NO→NO_2			9.04E-12	Peroxy radical operator
R2O2+HO_2→HO_2			1.49E-11	
R2O2+NO_3→NO_2			2.30E-12	
R2O2+MEO2→MEO2			2.00E-13	
R2O2+RO2_R→RO2_R			3.50E-14	
R2O2+R2O2→			3.50E-14	

ACPD

9, 22955–22992, 2009

Table 6. Continued.

Reactions	CB4	CB05	SAPRC-99	Comments
RO2_N+NO→NTR			9.04E-12	Peroxy radical operator
RO2_N+HO_2→ROOH			1.49E-11	
RO2_N+MEO2→HO_2+0.25MEOH+0.5MEK+0.5PROD2+0.75HCHO			2.30E-12	
RO2_N+NO_3→NO_2+HO_2+MEK			2.00E-13	
RO2_N+RO2_R→HO_2+0.5MEK+0.5PROD2			3.50E-14	
RO2_N+R2O2→RO2_N			3.50E-14	
RO2_N+RO2_N→MEK+HO_2+PROD2			3.50E-14	
RCO_O2+NO_2→PAN2			1.21E-11	Peroxy propionyl radicals
RCO_O2+NO→NO_2+ALD2+RO2_R			2.80E-11	
RCO_O2+HO_2→0.75RCO_OOH+0.25RCO_OH+0.25O_3			1.41E-11	
RCO_O2+NO_3→NO_2+ALD2+RO2_R			4.00E-12	
RCO_O2+MEO2→RCO_OH+HCHO			9.64E-12	
RCO_O2+RO2_R→RCO_OH			7.50E-12	
RCO_O2+R2O2→RCO_O2			7.50E-12	
RCO_O2+RO2_N→RCO_OH+PROD2			7.50E-12	
RCO_O2+C2O3→MEO2+ALD2+RO2_R			1.55E-11	
RCO_O2+RCO_O2→2ALD2+2RO2_R			1.55E-11	
BZCO_O2+NO_2→PBZN			1.37E-11	Peroxy radicals from aromatic aldehyde
PBZN→BZCO_O2+NO_2			3.12E-04	
BZCO_O2+NO→NO_2+BZ_O+R2O2			2.80E-11	
BZCO_O2+HO_2→0.75RCO_OOH+0.25RCO_OH+0.25O_3			1.41E-11	
BZCO_O2+NO_3→NO_2+BZ_O+R2O2			4.00E-12	
BZCO_O2+MEO2→RCO_OH+HCHO			9.64E-12	
BZCO_O2+RO2_R→RCO_OH			7.50E-12	
BZCO_O2+R2O2→BZCO_O2			7.50E-12	
BZCO_O2+RO2_N→RCO_OH+PROD2			7.50E-12	
BZCO_O2+C2O3→MEO2+BZ_O+R2O2			1.55E-11	
BZCO_O2+RCO_O2→ALD2+RO2_R+BZ_O+R2O2			1.55E-11	
BZCO_O2+BZCO_O2→2BZ_O+2R2O2			1.55E-11	
TBU_O+NO_2→NTR			2.40E-11	t-Butoxy radicals
TBU_O→ACET+MEO2			9.88E+02	
BZ_O+NO_2→NPHE			3.80E-11	Pheoxy radicals
BZ_O+HO_2→PHEN			1.49E-11	
BZ_O→PHEN			1.00E-03	
BZNO2_O+NO_2→			3.80E-11	Nitro-substituted phenoxy radicals
BZNO2_O+HO_2→NPHE			1.49E-11	
BZNO2_O→NPHE			1.00E-03	
NPHE+NO_3→HNO_3+BZNO2_O			3.78E-12	Nitrophenols
BACL→2C2O3			Photolysis	Biacetyl
BALD+HO→BZCO_O2			1.29E-11	Benzaldehyde
BALD→			Photolysis	
BALD+NO_3→HNO_3+BZCO_O2			2.62E-15	

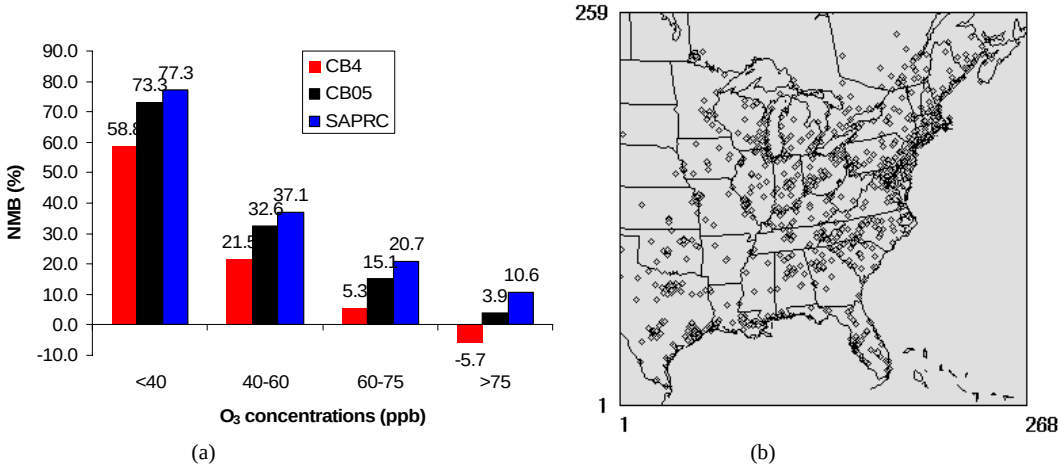

Fig. 1. **(a)** Comparison of the modeled (CB4, CB05 and SAPRC-99) and observed maximum 8-hour O_3 concentrations at the AIRNow monitoring sites: the NMB values of each model as a function of the observed maximum 8-h O_3 concentration ranges during the period of 15 July and 18 August, 2004; **(b)** the model domain and locations of AIRNow monitoring sites.

ACPD
9, 22955–22992, 2009

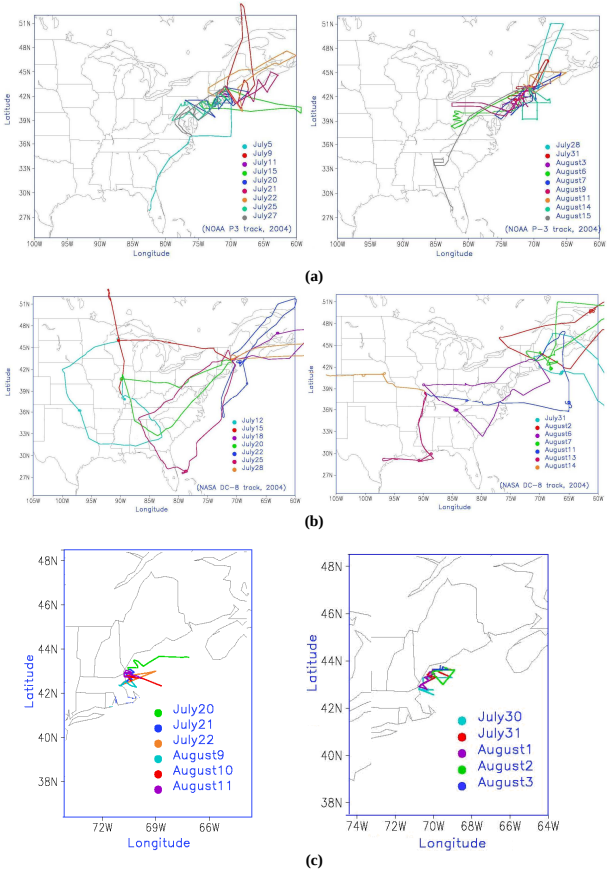

Fig. 2. Tracks of (**a**) P-3, (**b**) DC-8 and (**c**) ship tracks during the 2004 ICARTT period.

ACPD

9, 22955–22992, 2009

Eta-CMAQ air quality forecasts for O_3 and related species

S. Yu et al.

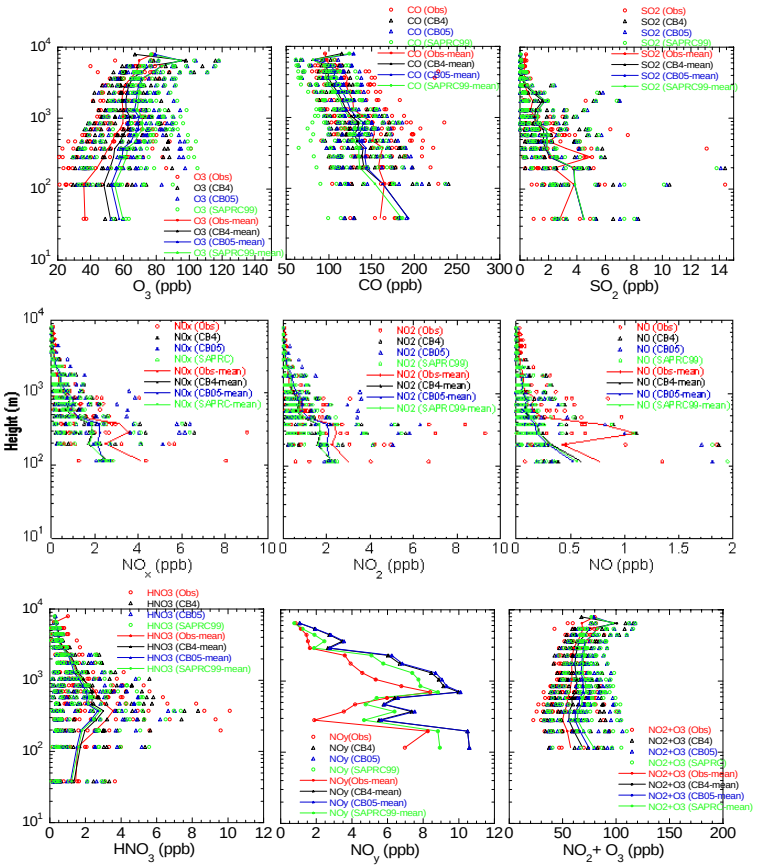

Fig. 3. Comparison of vertical O_3, CO, PAN, HNO_3, NO_y, NO_2+O_3 for the P-3 observations and models during 2004 ICARTT period. The solid lines represent the means of all data.

ACPD
9, 22955–22992, 2009

Eta-CMAQ air quality forecasts for O_3 and related species

S. Yu et al.

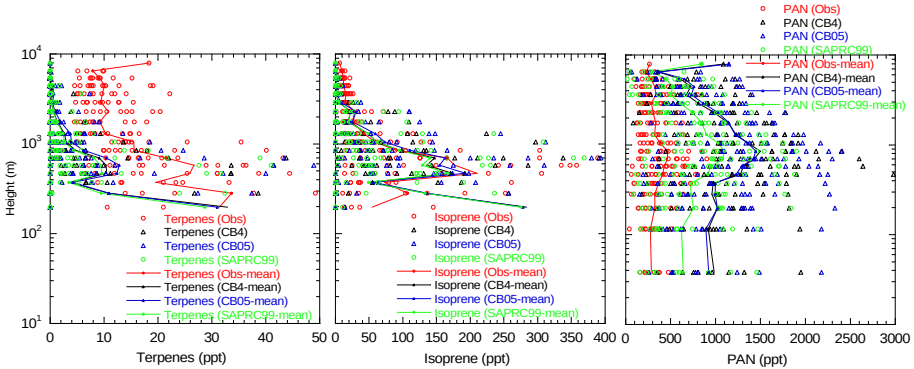

Fig. 4. Comparison of vertical terpenes, isoprene and PAN for the P-3 observations and models during 2004 ICARTT period.

ACPD
9, 22955–22992, 2009

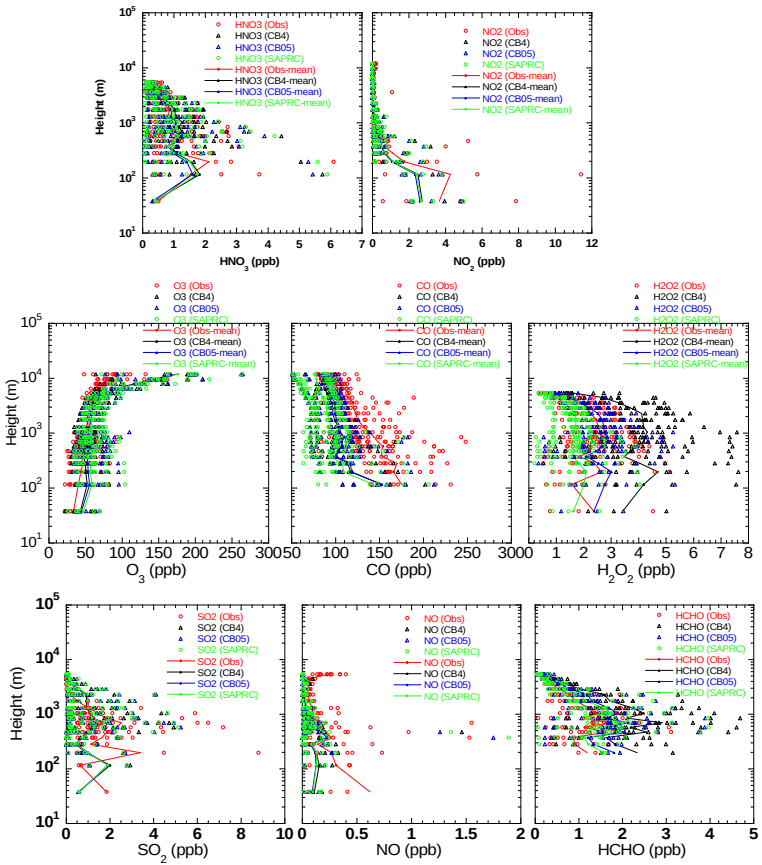

Fig. 5. The same as Fig. 3 but for vertical O_3, CO, H_2O_2, HNO_3, NO_2, NO, SO_2 and HCHO profiles based on DC-8.

ACPD
9, 22955–22992, 2009

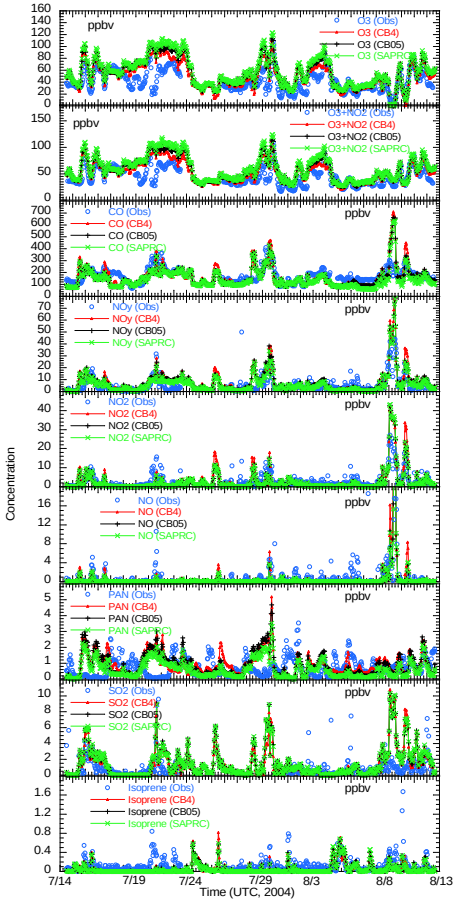

Fig. 6. Time series comparisons of model predictions and observations for different species on the basis of ship measurements.

ACPD

9, 22955–22992, 2009

Eta-CMAQ air quality forecasts for O_3 and related species

S. Yu et al.